Journal of
Applied Crystallography

ISSN 0021-8898

Received 5 January 2012
Accepted 13 June 2012

Mirror symmetries in multiple diffraction patterns of face-centred cubic crystals

Carlos Benedicto Ramos Parente,[a]* Vera Lucia Mazzocchi,[a] José Marcos Sasaki[b] and Lisandro Pavie Cardoso[c]

[a]Instituto de Pesquisas Energéticas e Nucleares (IPEN-CNEN/SP), São Paulo, SP, Brazil, [b]Universidade Federal do Ceará (UFC), Fortaleza, CE, Brazil, and [c]Universidade Estadual de Campinas (UNICAMP), Campinas, SP, Brazil. Correspondence e-mail: cparente@ipen.br

In this work, a study of the mirror symmetries appearing in multiple diffraction patterns of face-centred cubic crystals is carried out. Several different X-ray and neutron multiple diffraction patterns have been simulated for different face-centred cubic structures. The patterns were plotted in circular plots which showed that two types of symmetry mirrors coexist in the patterns: isomorphic and anamorphic mirrors. The number and types of mirrors depend on the *n*-fold symmetry of the scattering vector associated with the primary reflection. For *n* even, only *n* isomorphic mirrors appear in the patterns. For *n* odd, *n* isomorphic mirrors are formed intercalated between *n* anamorphic mirrors.

© 2012 International Union of Crystallography
Printed in Singapore – all rights reserved

1. Introduction

Periodicity in the appearance of peaks (or dips) in a multiple diffraction (m.d.) pattern is an intrinsic characteristic of such patterns. Since Renninger (1937) first produced experimental *Umweganregung* and *Aufhellung* patterns, it has been well known that such patterns are divided into sections. Each section appears as a mirror image of the neighbouring sections, and they repeat every certain number of degrees according to the *n*-fold symmetry operator associated with the scattering vector of the primary reflection. It is the same effect as placing mirrors between the sections. Examples of patterns exhibiting mirror symmetry are given by Renninger (1937, Figs. 2, 6, 8 and 10), Cole *et al.* (1962, Figs. 3 and 9), Moon & Shull (1964, Fig. 5), Soejima *et al.* (1985, Fig. 5), Chang (1984, Figs. 2.6, 6.1, 6.3a,b and 6.4a,b) and Chang (2004, Fig. 4.2).

Parente (1973) studied the neutron m.d. (NMD) obtained with the primary reflection 111 from an aluminium single crystal. The experimental *Aufhellung* pattern he measured had an extension sufficient to show two of the symmetry mirrors of the pattern. The experimental pattern he obtained can be seen in Fig. 5 of Parente & Caticha-Ellis (1974). This figure shows mirrors at 30 and 60° referred to an indexing scale. Clearly, the three peaks around 30° are positioned symmetrically and are equal in shape and intensity: one side is a mirror image of the other side. However, with the two peaks around 60° a quite different situation occurs: they are perfectly symmetrical in position but not in shape and intensity. At the time Parente (1973) reported the results of his work, it became clear to him that the lack of symmetry was a consequence of the fact that the secondary reflections were not produced by equivalent planes, except the planes (511) and (11$\bar{5}$). Different reflectivities imply different intensities. Sasaki (1993) observed the same effect in an X-ray m.d. (XMD) pattern obtained with Cu $K\alpha_1$ radiation and primary reflection 222 from a gallium arsenide (GaAs) single crystal. Two symmetrical peaks of the GaAs(222) *Umweganregung* (*Umweg*) pattern having different intensities are shown in Fig. 1. Indexing in the figure corresponds to the coupling between the secondary reflections producing the peaks and the primary reflection.

According to Chang (1984), the appearance of mirror symmetries in an m.d. pattern depends on the symmetry of the rotation vector used to produce the pattern. According to this author, an expression can be used as a general rule for predicting the angular repetition of the mirror symmetries. The number of symmetry mirrors is given by

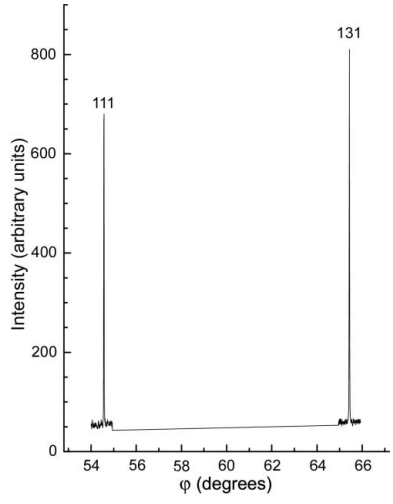

Figure 1
Two symmetrical peaks having different intensities observed by Sasaki (1993) in an experimental XMD pattern, obtained with reflection 222 from a GaAs single crystal.

$$n_{\rm M} = n_{\rm r}(p)R. \quad (1)$$

In expression (1), $n_{\rm r}(p)$ is the n-fold symmetry of the rotation vector set along the scattering vector of the primary reflection. Thus, $n_{\rm M}$ depends on the particular primary reflection chosen for the experiment. R is a rotation operator, which is equal to 2 in order to take into account that, in a full rotation (360°), a reciprocal lattice point (RELP) enters and leaves the surface of the Ewald sphere, except in those incidental cases where the RELP trajectory touches the surface at just one point. According to equation (1), for two-, three- and fourfold rotation axes the m.d. patterns show four-, six- and eightfold mirror symmetries, respectively. Chang (1984) also mentioned that, in an XMD pattern of Ge(222), symmetry mirrors occur every 30°. It is explained that, although the threefold symmetry of direction ⟨222⟩ should generate a sixfold symmetry, the existence of a pair of tetrahedrons differing by 60° generates mirrors every 30°. This author further pointed out that ambiguity is often encountered in indexing m.d. patterns obtained with crystals involving high symmetry, as is the case mentioned above. Chang & Caticha-Ellis (1978) proposed an experimental way to overcome this problem, although reporting of the solution found by these authors is beyond the scope of this work. It should be mentioned that, in a second book dealing with the theory and application of multiple diffraction, Chang (2004) again refers to the ambiguity and difficulty of indexing m.d. patterns obtained with crystals involving high symmetry.

2. Simulated m.d. patterns

The main goal of this work is a systematic search for mirror symmetries in NMD and XMD patterns of face-centred cubic (f.c.c.) crystals. We have carried out an investigation of such symmetries by simulating m.d. patterns for different primary reflections from different f.c.c. crystals. NMD patterns were simulated by the computer program *MULTI* (Mazzocchi, 1984). This program was used by Mazzocchi & Parente (1994, 1998) and Campos *et al.* (2010) with quite good results. XMD patterns were simulated by *MULTX*, a program derived from *MULTI*. Quite good results were obtained with *MULTX* by Salles da Costa *et al.* (1990, 1992).

Figs. 2(*a*) and 2(*b*) were prepared to show the relationships between peak intensities and reflectivities. They are composed of simulated peaks and some reflectivity curves involved in the formation of such peaks. We choose the interactions between the primary beam and all the secondary beams. Other interactions, such as for example those between the incident and the secondary beams, would serve for this purpose as well. According to Parente *et al.* (1994), each beam interacts with the $n-1$ other beams producing $n(n-1)$ interactions, where n is the total number of beams involved in the formation of a peak. The patterns in Figs. 2(*a*) and 2(*b*) were simulated for the 111 primary reflection of a cylindrical aluminium single crystal around φ equal to 30 and 60°, respectively. Intensities were plotted as the ratio $\Gamma = P_{1,\rm m}/P_{1,\rm s}$, where $P_{1,\rm m}$ and $P_{1,\rm s}$ are the power of the primary beam when, respectively, multiple and single diffraction occur. The data for the reflectivity curves were also calculated by the program. The wavelength was assumed to be the same as that used by Parente (1973), namely λ = 1.1027 Å. In order that simulated and experimental peaks look alike, the mosaic breadth was assumed to be equal to that found for the real aluminium crystal, namely $\eta = 0.144°$ (0.0025 rad). Only the crystal shapes were different: the crystal used for the experimental results was a 3 × 3 × 1 inch (1 inch = 25.4 mm) plate, and in the simulations it was assumed to be a 3 inch diameter × 1 inch height disc. In both crystals, the ⟨111⟩ direction was orthogonal to the basis. By comparing the simulated peaks of Fig. 2 with the corresponding experimental peaks in Fig. 5 of Parente & Caticha-Ellis (1974), one verifies that there is a great similitude between them. Comparing the peaks with the reflectivity curves in Fig. 2, it becomes clear why those around 30° are perfectly symmetrical while those around 60° are not.

Table 1 was prepared with data given in the output of *MULTI*, when calculating the peaks and curves in Fig. 2.

In the table, the peaks on the left are aligned with those on the right, forming pairs of peaks whose intensities result from

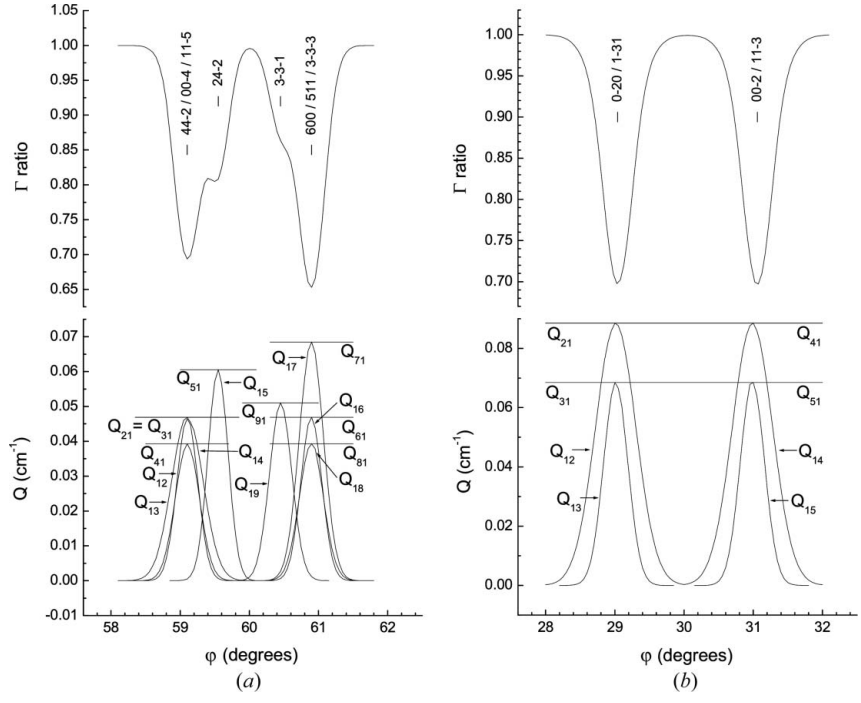

Figure 2
Simulated NMD peaks for Al(111) around mirrors placed at 60° (*a*) and 30° (*b*). Reflectivity curves for the interactions between the primary beam (numbered 1) and the secondary beams (numbered 2–9) are also shown.

Table 1
Main characteristics of the secondary beams producing the peaks of Figs. 2(*a*) and 2(*b*).

$Q_{ij\ \max}$ and Q_{ji} correspond to the interactions between the primary and the secondary beams involved in the formation of the peaks.

hkl	*j*	$j_{\max}$ (°)	$Q_{1j\ \max} = Q_{j1}$ (cm^{-1})	C_Z	Beam type	$\overline{\ell}$ (cm)	*hkl*	*j*	$j_{\max}$ (°)	$Q_{1j\ \max} = Q_{j1}$ (cm^{-1})	C_Z	Beam type	$\overline{\ell}$ (cm)
$44\overline{2}$	2	59.10	0.04688	−0.70757	R	2.48	600	6	60.90	0.04688	−0.70757	R	2.48
$00\overline{4}$	3	59.10	0.04688	0.86481	T	2.31	511	7	60.90	0.06848	−0.86481	R	2.31
$11\overline{5}$	4	59.10	0.03930	0.70757	T	2.48	$3\overline{3}3$	8	60.90	0.03930	0.70757	T	2.48
$24\overline{2}$	5	59.55	0.06053	−0.39310	R	3.20	$3\overline{3}1$	9	60.45	0.05103	0.39310	T	3.20
$0\overline{2}0$	2	29.01	0.08851	0.55034	T	2.77	$00\overline{2}$	4	30.99	0.08851	0.55034	T	2.77
$1\overline{3}1$	3	29.01	0.06848	0.39310	T	3.20	$11\overline{3}$	5	30.99	0.06848	0.39310	T	3.20

secondary beams with equal path lengths. This allows a comparison between the main characteristics of the reflections involved in the formation of the peaks (Parente *et al.*, 1994). These characteristics are the Miller indices of the secondary reflections (*hkl*), the maximum reflectivity for an interaction $1 \rightarrow j$ between the primary beam and one secondary beam ($Q_{1j\ \max}$), which is equal to the (constant) reverse interaction $j \rightarrow 1$ between the secondary beam and the primary beam (Q_{j1}), the direction cosines of the beams relative to the normal to the primary planes (C_Z), the beam type (R reflected, T transmitted) and the effective path length of the beam ($\overline{\ell}$). The number assigned to each reflection (j) and the positions of the peak maximum intensities ($\varphi_{\max}$) are also listed. For the peaks related to the mirror at $\varphi = 60°$, $Q_{1j\ \max}$, C_Z and beam type are different for the reflections in the pairs $00\overline{4}$/511 and $24\overline{2}$/$3\overline{3}1$. Differences are observed in Fig. 2(*a*) for these two pairs when comparing the reflectivity curves. It should be noted that for the pairs $44\overline{2}$/600 and $11\overline{5}$/$3\overline{3}3$ the reflections have equal characteristics. For the peaks related to the mirror at $\varphi = 30°$ the reflections in the two pairs formed exhibit a perfect equality in their characteristics. That is the reason why the two peaks in Fig. 2(*b*) are exactly equal. It should be noted that, in this case, the two pairs are formed by equivalent reflections in the cubic system.

The simulations plotted in Figs. 3(*a*) and 3(*b*) were carried out in order to verify if the characteristics observed in Figs. 2(*a*) and 2(*b*), respectively, change with changes in a few parameters given as input in the program *MULTI*. The simulations were obtained by varying the radius (r) and height (h) of the single crystal, and its mosaic spread (η). In Fig. 3(*a*), the peaks change their shapes and intensities in an extraordinary way. One can easily verify that η plays a more important role in the modifications of shape and intensity than r or h does. On the other hand, in Fig. 3(*b*), with an identical variation of parameters, the peaks remain rigorously symmetrical although a great variation in shape and intensity still occurs.

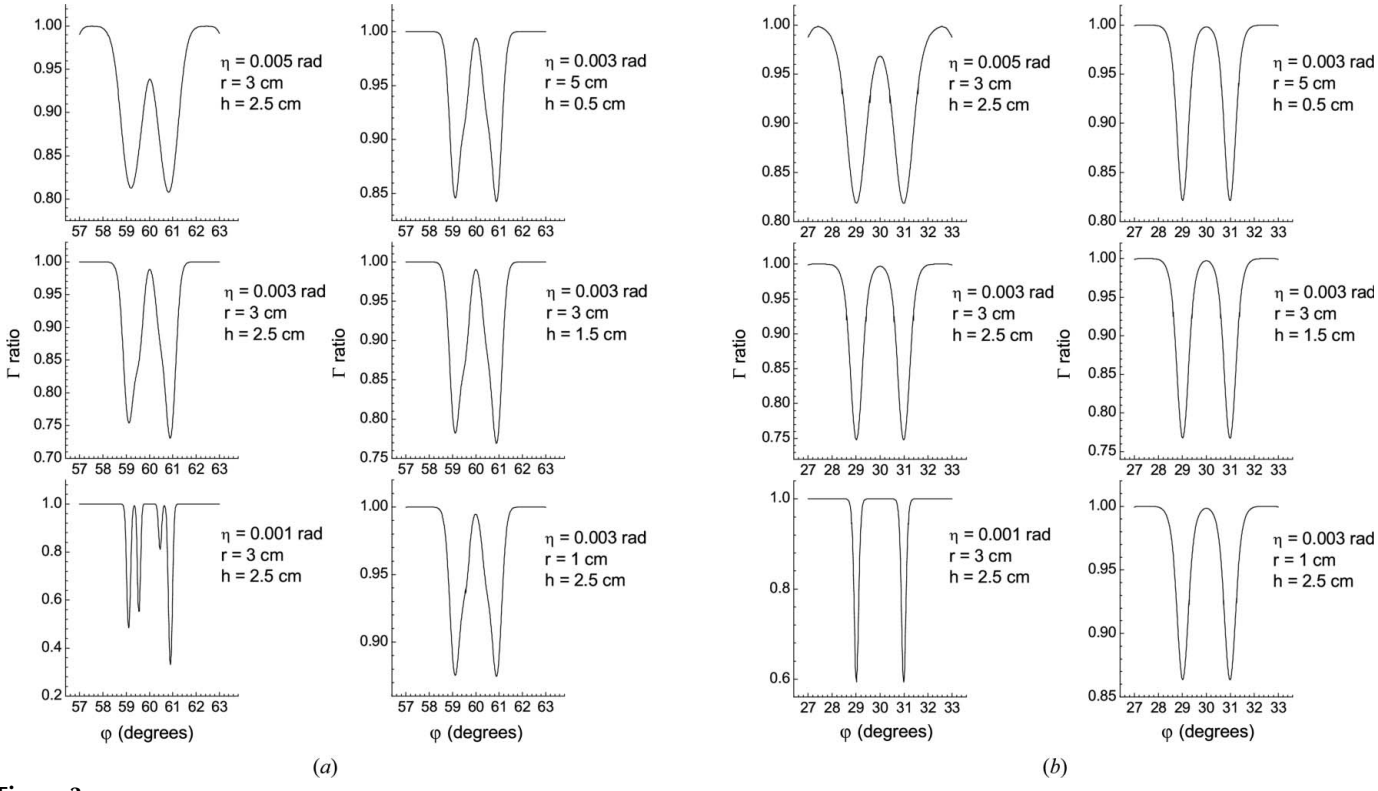

Figure 3
Changes in the shape and intensity of simulated peaks around mirrors placed at 60° (*a*) and 30° (*b*) with a variation of r, h and η.

For a mirror like that at 30° we adopt the name 'isomorphic mirror' (IM). It produces only pairs of fully symmetrical peaks. We call a mirror like that at 60° an 'anamorphic mirror' (AM). It produces pairs of symmetrically positioned peaks having different intensities and shapes amongst pairs of fully symmetrical peaks. It is worth mentioning that, depending on some sample characteristics, unsymmetrical peaks can appear with such minute differences that they can be misinterpreted as being symmetrical, particularly in experimental patterns.

We have also simulated NMD and XMD patterns in a full extension of the azimuthal angle φ, *i.e.* for φ ranging from 0 to 360°. We have plotted such patterns in circular plots (Figs. 4–11). A circular plot allows a better visualization of the mirror symmetry associated with the n_r-fold symmetry of the primary reflection. In a circular plot, the intensity axis is radial and the φ axis circular. It should be noted that no intensity scale is shown in our plots. We thought that it was not necessary to include such a scale since our main goal is to show the mirror

Table 2
List of the simulated patterns with their characteristics.

Crystal	Space group	Primary reflection	Symmetry (n_r-fold)	Pattern type	Mirrors	Notes
Al	*Fm*3*m*	111	3	*Aufhellung*	3 IM, 3 AM	NMD, Fig. 4
		220	2	Mixed	2 IM	NMD, Fig. 5
		042	1	Mixed	1 IM, 1 AM	NMD, Fig. 6
Si	*Fd*3*m*	311	1	Mixed	1 IM, 1 AM	NMD, Fig. 7
		622	1	*Umweg*	1 IM, 1 AM	XMD, Fig. 8
		222	3	*Umweg*	3 IM, 3 AM	XMD, Fig. 9
GaAs	$F\bar{4}3m$	002	4	*Umweg*	4 IM	XMD, Fig. 10
		222	3	*Umweg*	3 IM, 3 AM	XMD, Fig. 11

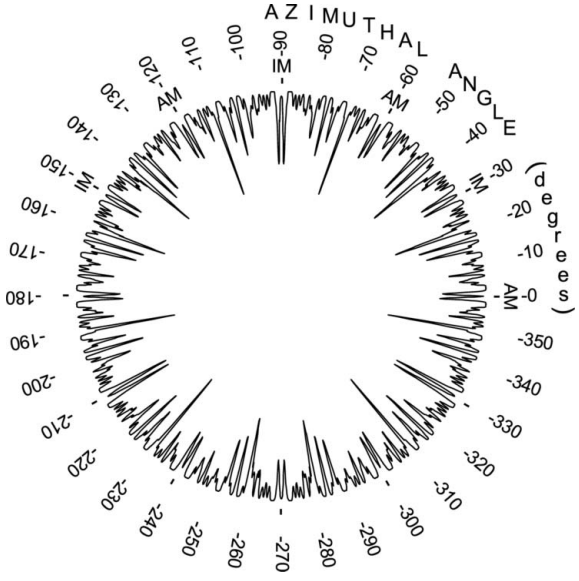

Figure 4
Simulated NMD pattern for Al(111).

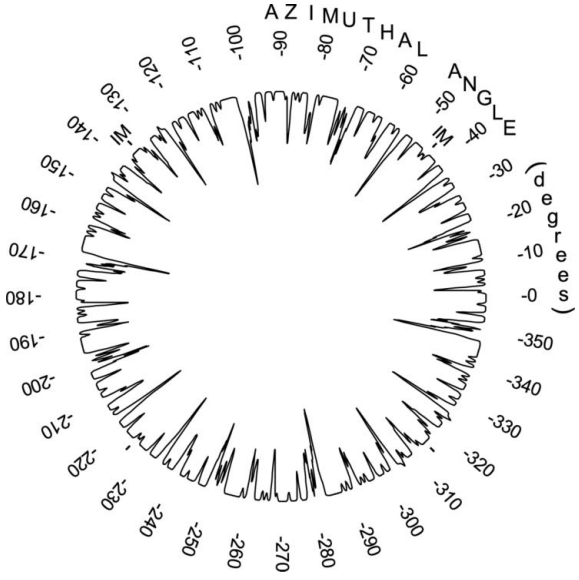

Figure 5
Simulated NMD pattern for Al(220).

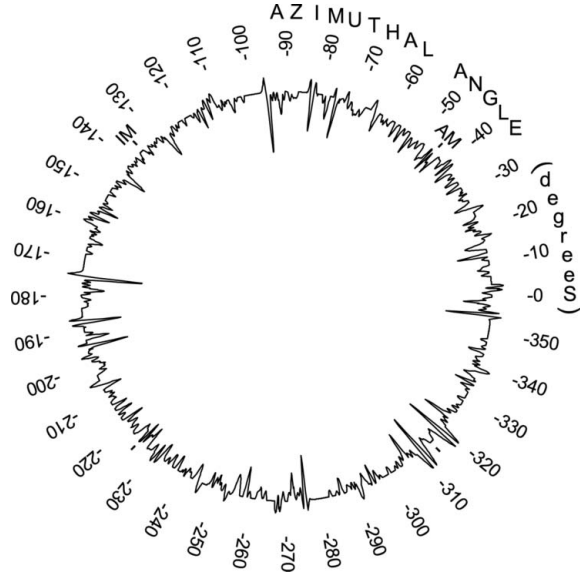

Figure 6
Simulated NMD pattern for Al(042).

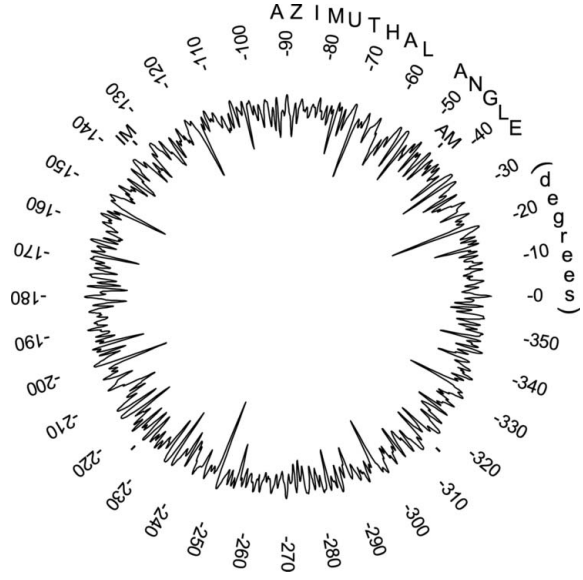

Figure 7
Simulated NMD pattern for Si(311).

symmetries and they become evident by a simple observation of the plots.

Table 2 lists the patterns we have simulated. For each one is given the crystalline structure of the element or compound, the space group, the primary reflection assumed, the n_r-fold symmetry associated with the primary reflection, the pattern type (according to Mazzocchi & Parente, 1994), and the number and type of the mirrors present in the plot. Information on whether the plot was simulated as an NMD or XMD pattern and the number of the corresponding figure are also included in Table 2. The neutron wavelength assumed in the simulations was $\lambda = 1.1027$ Å, and in the case of X-rays the wavelength of the Cu $K\alpha_1$ radiation was adopted.

3. Conclusions

When $n_r(p)$ is even in expression (1) only IMs are observed in the plot. In this case, the number of IMs (m_I) is equal to that given by equation (1), *i.e.* $m_I = n_M$. When $n_r(p)$ is odd both AMs and IMs appear. Mirrors of one type intercalate into mirrors of the other type, in a regular sequence. The number of AMs (m_A) is also equal to n_M, *i.e.* $m_A = n_M = m_I$. Of course, the total number of mirrors (m_T) is given by $m_T = m_I + m_A$, where $m_A = 0$ when $n_r(p)$ is even.

As can be readily seen in Figs. 4–11, each simulated circular plot forms a figure that follows the n_r-fold symmetry of the crystalline direction associated with the scattering vector of the primary reflection. If a circular plot is folded along an IM

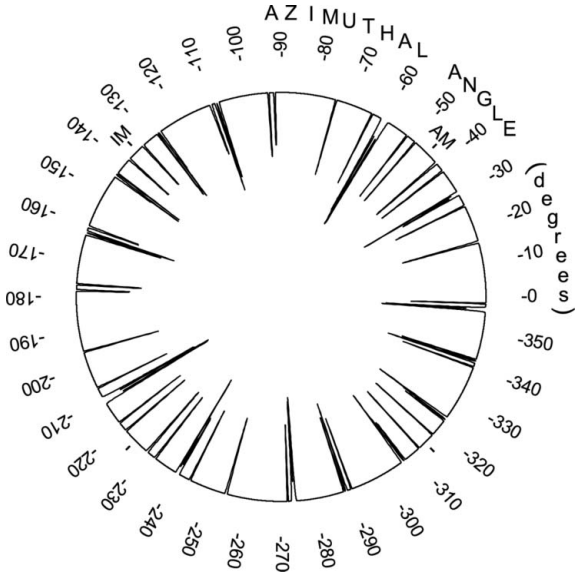

Figure 8
Simulated XMD pattern for Si(622).

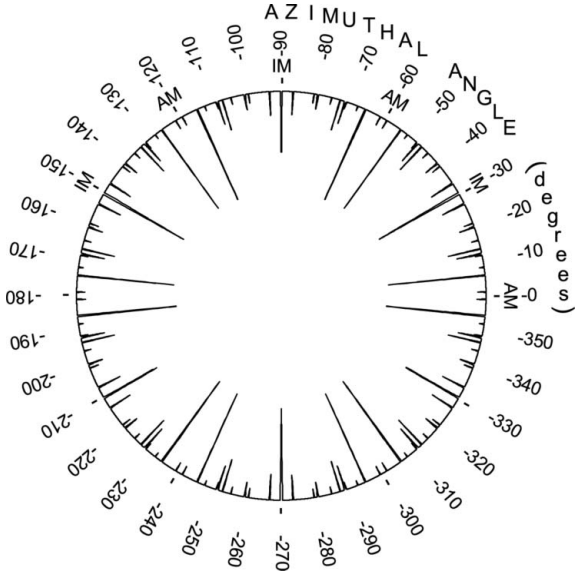

Figure 9
Simulated XMD pattern for Si(222).

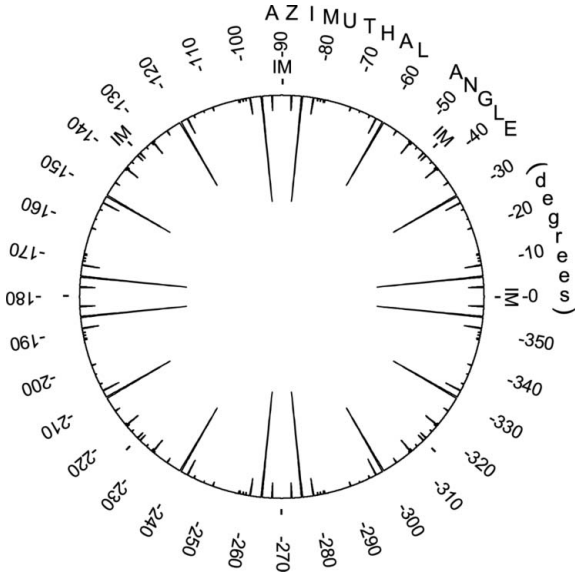

Figure 10
Simulated XMD pattern for GaAs(002).

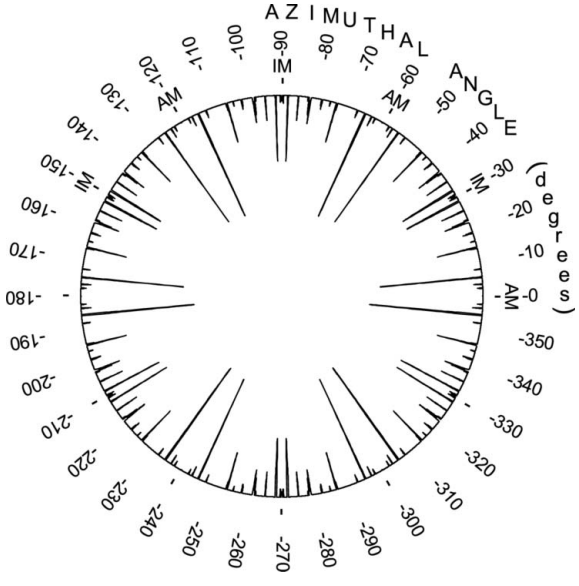

Figure 11
Simulated XMD pattern for GaAs(222).

the peaks on one side will perfectly match those on the opposite side. If the fold is along an AM there will be peaks that do not match. Clearly, the same occurs in the case of a linear plot.

Finally, it should be noted that, in a linear plot, m_T is twice that of a circular plot. This means that, in equation (1), R must be equal to 2 for a linear plot (see §1) and equal to 1 for a circular plot. In a circular plot, a mirror passing through a certain azimuthal position also passes through a position 180° apart, irrespective of whether it is an IM or AM.

References

Campos, L. C. de, Parente, C. B. R. & Mazzocchi, V. L. (2010). *J. Appl. Cryst.* **43**, 1488–1494.

Chang, S.-L. (1984). *Multiple Diffraction of X-rays in Crystals.* Berlin, Heidelberg, New York, Tokyo: Springer-Verlag.

Chang, S.-L. (2004). *X-ray Multiple-Wave Diffraction: Theory and Application.* Springer Series in Solid State Sciences, Vol. 143. Berlin, Heidelberg, New York: Springer-Verlag.

Chang, S.-L. & Caticha-Ellis, S. (1978). *Acta Cryst.* A**34**, 825–826.

Cole, H., Chambers, F. H. & Dunn, H. M. (1962). *Acta Cryst.* **15**, 138–144.

Mazzocchi, V. L. (1984). MSc dissertation, Universidade de São Paulo (Usp), São Paulo, SP, Brazil.

Mazzocchi, V. L. & Parente, C. B. R. (1994). *J. Appl. Cryst.* **27**, 475–481.

Mazzocchi, V. L. & Parente, C. B. R. (1998). *J. Appl. Cryst.* **31**, 718–725.

Moon, R. M. & Shull, C. G. (1964). *Acta Cryst.* **17**, 805–812.

Parente, C. B. R. (1973). PhD thesis, Universidade de São Paulo (Usp), São Paulo, SP, Brazil.

Parente, C. B. R. & Caticha-Ellis, S. (1974). *Jpn. J. Appl. Phys.* **13**, 1506–1513.

Parente, C. B. R., Mazzocchi, V. L. & Pimentel, F. J. F. (1994). *J. Appl. Cryst.* **27**, 463–474.

Renninger, M. (1937). *Z. Phys.* **106**, 141–176.

Salles da Costa, C. A. B., Cardoso, L. P., Mazzocchi, V. L. & Parente, C. B. R. (1990). *Defect Control in Semiconductors*, Vol. II, *Proceedings of the International Conference on the Science and Technology of Defect Control in Semiconductors*, edited by K. Sumino, pp. 1535–1539. Amsterdam: Elsevier.

Salles da Costa, C. A. B., Cardoso, L. P., Mazzocchi, V. L. & Parente, C. B. R. (1992). *J. Appl. Cryst.* **25**, 366–371.

Sasaki, J. M. (1993). PhD thesis, Universidade Estadual de Campinas (UNICAMP), Campinas, SP, Brazil.

Soejima, Y., Okazaki, A. & Matsumoto, T. (1985). *Acta Cryst.* A**41**, 128–133.